

Macroscopic effects of local oxygen fluctuations in $\text{YBa}_2\text{Cu}_3\text{O}_{6+x}$

P. A. Rikvold

*Department of Physics B-159 and Center for Materials Research and Technology B-159
and Supercomputer Computations Research Institute B-186, Florida State University, Tallahassee, Florida 32306-3016*

M. A. Novotny

Supercomputer Computations Research Institute B-186, Florida State University, Tallahassee, Florida 32306-4052

T. Aukrust

IBM Bergen Scientific Centre, Thormøhlensgate 55, Bergen High Technology Centre, N-5008 Bergen, Norway

(Received 8 May 1990)

Recent experimental studies of the high-temperature superconductor $\text{YBa}_2\text{Cu}_3\text{O}_{6+x}$ at high temperatures (above 700 K) detect a maximum in the derivative with respect to oxygen chemical potential of the stoichiometric factor x , located within the disordered tetragonal-phase region. Here we present approximate numerical calculations by a new mean-field technique, which explain this macroscopic effect in terms of local, essentially one-dimensional, fluctuations in the distribution of oxygen atoms in a lattice-gas model for the Cu-O basal planes of this material. Such fluctuations are characteristic of a system near a disorder line in its phase diagram, and are associated with the formation of finite fragments of positionally and orientationally disordered oxygen chains. Our calculations agree with the positions and widths of the experimentally observed maxima, and also predict corresponding peaks in the specific heat. The mean-field results are complemented with large-scale Monte Carlo and numerical transfer-matrix calculations for the same model. The finite-size scaling behavior of the local-fluctuation peaks in the Monte Carlo data is distinctly different from that of the peaks which correspond to phase transitions. The physical picture developed in this study also provides an alternative to the low-density, low-temperature orthorhombic phase that has been proposed by other authors.

I. INTRODUCTION

In a recent thermodynamic study of the oxygen content of the high-temperature superconductor $\text{YBa}_2\text{Cu}_3\text{O}_{6+x}$, McKinnon *et al.*¹ observed a low, broad maximum in the derivative of the stoichiometric factor x with respect to the oxygen chemical potential. This maximum was located within the disordered tetragonal (non-superconducting) phase region, and was clearly distinguishable from the peak which signals the tetragonal-to-orthorhombic phase transition. Similar maxima in this quantity, as well as in the specific heat, have also been seen in numerical Monte Carlo^{2,3} and transfer-matrix³ calculations. Here we present, in addition to further Monte Carlo and transfer-matrix results, approximate numerical calculations by a new mean-field technique, which explain these observations in terms of short-range order and anisotropy in the distribution of oxygen atoms in a lattice-gas model of the Cu-O basal planes. Such local anisotropy appears when the oxygen concentration is sufficiently high to allow formation of oxygen chains due to attractive effective interactions between pairs of O atoms connected by a Cu atom, but too low for the formation of an ordered orthorhombic phase. Although no thermodynamic singularities (phase transitions) are associated with these local fluctuations, their effects are

nevertheless macroscopically observable, as illustrated by the above-mentioned experimental and numerical observations. Our approximation method, which is described in Sec. III, is based on the similarity between these local, essentially one-dimensional, fluctuations and the fluctuations characteristic of a system near a *disorder point*.⁴⁻⁶ Disorder lines, which are lines of disorder points, exist within the disordered regions of the phase diagrams for a number of anisotropic lattice-gas models with competing interactions. Much of the inspiration for the present work arises from Gompper and Schick's successful application of the disorder-line concept to explain the unusual macroscopic properties of microemulsions.^{7,8}

The purpose of this study is twofold. First, we aim to give a microscopic physical picture of the fluctuations that produce the experimentally observed maxima in thermodynamic response functions.¹ Second, we argue that this picture also provides an alternative to the low-density, low-temperature orthorhombic phase that has been proposed by other authors.^{2,9-12}

II. MODEL

The lattice-gas model of the Cu-O basal planes was originally introduced by Berera, de Fontaine, Moss, and Wille^{13,14} and investigated in a number of recent

studies.^{3,9,15-19} Its relevance to the physical materials has recently been reviewed.^{20,21} The basal planes consist of a square lattice of copper atoms with lattice constant a and a basis of two oxygen sites at $(\frac{a}{2}, 0)$ and $(0, \frac{a}{2})$. The O atoms interact through repulsive nearest-neighbor and locally anisotropic next-nearest-neighbor effective interactions. The Hamiltonian is

$$\mathcal{H} - \mu N_a = -\Phi_{\text{NN}} \sum_{\langle \text{NN} \rangle} c_i c_j - \Phi_{\text{Cu}} \sum_{\langle \text{NNN}_{\text{Cu}} \rangle} c_i c_j - \Phi_{\text{V}} \sum_{\langle \text{NNN}_{\text{V}} \rangle} c_i c_j - \mu \sum_i c_i. \quad (1)$$

Here the c_i are the site-occupation variables for the O atoms; $c_i = 1$ if site i is occupied, and $c_i = 0$ if site i is empty. Φ_{NN} is the effective nearest-neighbor (NN) interaction energy, and Φ_{Cu} and Φ_{V} are the effective next-nearest-neighbor (NNN) interaction energies, with and without a Cu atom between the O sites, respectively. The sums run over all the indicated pairs of sites. The oxygen chemical potential is μ , and N_a is the total number of O atoms. The basal-plane lattice and the interactions in the Hamiltonian are shown in Fig. 1. We use dimensionless units such that $\Phi_{\text{NN}} = -1$ (repulsive), and choose $\Phi_{\text{V}} = -0.5$ (repulsive), and $\Phi_{\text{Cu}} = +0.5$ (attractive). These interactions were also used in previous numerical studies,^{3,9,14-19} and yield a phase diagram in reasonable agreement with experiments.^{1,22} For direct quantitative comparison with the experimental isotherm at $T = 923$ K, measured by McKinnon *et al.*,¹ we have also performed some calculations with the effective interaction constants recently obtained in a first-principles linear muffin-tin orbital (LMTO) calculation by Sterne and

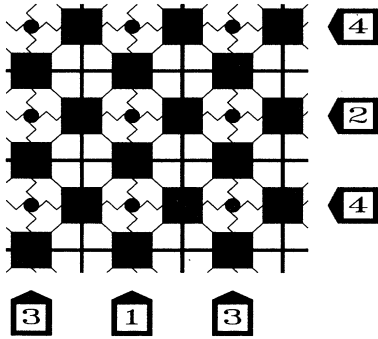


FIG. 1. The lattice in the basal Cu-O planes, and the interactions in the lattice-gas Hamiltonian, Eq. (1), are illustrated. The circles represent Cu atoms, and the squares represent O sites. The nearest-neighbor interactions (Φ_{NN}) are shown as thin diagonal lines, the next-nearest-neighbor interactions through a copper (Φ_{Cu}) and through a vacancy (Φ_{V}) are shown respectively as zig-zag lines and thick solid lines. The numbered arrows indicate the one-dimensional chains of O sites connected by Cu atoms. The odd-numbered chains “1” and “3” are vertical in the figure, and the even-numbered chains “2” and “4” are horizontal.

Wille.²³ The oxygen concentration in the basal planes, Θ , is half of the factor x in the stoichiometric formula $\text{YBa}_2\text{Cu}_3\text{O}_{6+x}$,

$$\Theta = \frac{N_a}{N} = \frac{1}{N} \sum_{i=1}^N c_i = \frac{x}{2}, \quad (2)$$

where N is the total number of O sites. The quantity

$$\chi_{\Theta} = \left(\frac{d\Theta}{d\mu} \right)_T, \quad (3)$$

which is half of the thermodynamic response function measured by McKinnon *et al.*,¹ is identical to the nonordering susceptibility for the equivalent Ising model. At low temperatures both the experimental and theoretical phase diagrams contain three phases: A disordered tetragonal phase with $\Theta \simeq 0$ (denoted tetra-0), and two ordered orthorhombic phases with $\Theta \simeq 1/4$ (denoted ortho-1/4) and $\Theta \simeq 1/2$ (denoted ortho-1/2), respectively. At temperatures above approximately 800 K the ortho-1/4 phase becomes unstable, leaving only the tetra-0 and ortho-1/2 phases. Detailed phase diagrams, based on numerical transfer-matrix and Monte Carlo calculations, have been presented in Refs. 3 and 9.

III. CHAIN MEAN-FIELD (CMF) APPROXIMATION

The enhanced local fluctuations that give rise to the observed maxima in the nonordering susceptibility χ_{Θ} and the specific heat C are associated with the formation of finite oxygen chains due to the attractive interaction Φ_{Cu} , and are basically one dimensional in character. Such one-dimensional fluctuations are characteristic of *disorder points*, which are points in a phase diagram where short-range correlations change their qualitative behavior.⁴⁻⁶ One of the characteristics of a system at a disorder point is that correlation functions along certain symmetry directions (which depend on the details of the lattice and the interactions) become identical in form to the (exactly known) correlation function of the one-dimensional Ising (lattice-gas) model in zero magnetic field.^{4,6} It is this particular aspect of the disorder-line concept that we have used to develop the mean-field approximation described below.

The basic idea of our approximation is to treat the correlations *along* the oxygen chains in the Cu-O basal planes exactly, whereas chain-chain interactions are taken into account in a self-consistent manner. For this we use a mean-field approximation in which the exactly treated subsystems are the one-dimensional chains that consist of next-nearest-neighbor oxygen sites connected by copper atoms. With the different emphasis of obtaining an improved mean-field approximation for studying phase transitions, a similar approach has previously been applied to weakly coupled chainlike magnetic systems.²⁴⁻²⁷ One of the Cu-O planes with the fourfold degenerate chains is shown in Fig. 1. The chains tha.

are vertical in the figure are numbered “1” and “3”, and those that are horizontal are numbered “2” and “4”. As usual in mean-field theories, the condition that the equilibrium state corresponds to a minimum in the free energy is equivalent to a set of coupled nonlinear equations for the *effective* chemical potentials μ_α that act on each of the subsystems. For a vertical chain labeled “1” this equation is

$$\mu_1 = \mu + 2\Phi_{\text{NN}}[\tilde{\Theta}(\mu_2) + \tilde{\Theta}(\mu_4)] + 2\Phi_{\text{V}}\tilde{\Theta}(\mu_3) - 2\Phi_{\text{NN}} - \Phi_{\text{V}}, \quad (4)$$

$$\tilde{\Theta}(\mu_\alpha) = \frac{1}{2} \left\{ \tanh \left(\frac{\mu_\alpha - \mu_0}{2k_B T} \right) \left[1 - \frac{1 - \exp(-\Phi_{\text{Cu}}/k_B T)}{\cosh^2 \left(\frac{\mu_\alpha - \mu_0}{2k_B T} \right)} \right]^{-1/2} + 1 \right\}. \quad (5)$$

The quantity $\mu_0 = -2\Phi_{\text{NN}} - \Phi_{\text{Cu}} - \Phi_{\text{V}}$ is the value of the chemical potential about which the phase diagram is symmetric (corresponding to zero magnetic field in the equivalent Ising model).²⁸ The numbering of the four subsystems is of course arbitrary. The “vertical” chains were chosen as those subject to the largest effective fields, and the chain numbers were assigned so that the condition $\mu_1 \geq \mu_3 \geq \mu_2 \geq \mu_4$ was satisfied.

For *weakly* coupled chain systems this method provides excellent estimates of the critical temperatures.²⁴ In our present case the chains are not weakly coupled, and we find numerically only a slightly improved T_c , compared to the simplest mean-field approximation. However, our main interest is to study the *local* fluctuations that lead to the formation of short fragments of oxygen chains in the disordered phase, and thus to the breaking of *local* isotropy. To prevent the system from settling into the disordered, isotropic equilibrium phase, in which the four subsystems are equivalent, we therefore apply weak, symmetry-breaking chemical potentials that are different for each of the four subsystems. We find that the resulting anisotropic “constrained equilibrium” state is quite insensitive to the strengths and details of these symmetry-breaking chemical potentials. The parts of χ_Θ and C that correspond to the local fluctuations were obtained as averages in this constrained state of the susceptibility and specific heat of the four one-dimensional subsystems, each acted on by its respective effective chemical potential μ_α . (Although it is easy to obtain the specific heat and susceptibility in closed form by differentiating the exact expression for the chain free energy,²⁸ numerical evaluation of the former requires the determination of small quantities by subtraction of much larger ones. In practice we therefore found it more reliable to evaluate the specific heat by numerical differentiation of the exact free energy.)

IV. RESULTS AND DISCUSSION

Our main numerical results are shown in the figures. The data displayed in Figs. 2–4 were obtained with the

where the coupling to the horizontal chains is through Φ_{NN} , and to the vertical chains labeled “3” through Φ_{V} . The equation for μ_3 is obtained by interchanging the subscripts “1” and “3”. The effective fields μ_2 and μ_4 which act on the horizontal chains, are obtained from μ_1 and μ_3 by interchanging even and odd indices. In these equations the subsystem oxygen concentrations $\tilde{\Theta}(\mu_\alpha)$ are given by the exact concentration of a one-dimensional lattice gas with interaction constant Φ_{Cu} , subject to a chemical potential μ_α ,

dimensionless interaction constants given after Eq. (1), $\Phi_{\text{NN}} = -1$, $\Phi_{\text{V}} = -0.5$, and $\Phi_{\text{Cu}} = +0.5$. Fig. 2(a) shows the specific heat per site $C/(Nk_B)$ versus chemical potential $\mu/|\Phi_{\text{NN}}|$ at temperature $k_B T/|\Phi_{\text{NN}}| = 0.175$. (With the overall energy scale adjusted to yield a phase diagram in agreement with the experimental data of Specht *et al.*,²² as in Ref. 3, this dimensionless temperature corresponds to approximately 640 K.) The solid line represents the contribution from local fluctuations, obtained with the chain mean-field (CMF) method described above, whereas the data points are Monte Carlo results for the full specific heat of $2(L \times L)$ systems with $L = 8, 16$, and 32 . The local contribution shows two pairs of maxima, one near each of the two phase transitions that involve the ortho-1/4 phase. This double-peak structure corresponds to that of the exact specific heat for the one-dimensional Ising model, which has two narrowly spaced maxima symmetrically located about zero magnetic field. Of the two CMF maxima near the tetra-0-to-ortho-1/4 transition, the larger one lies well inside the disordered phase region, whereas the smaller one lies close to the transition itself. The maximum within the disordered region coincides with a maximum in the Monte Carlo data, whose height does not scale with the system size L . Near the ortho-1/4-to-ortho-1/2 transition a similar situation is seen, with the nonscaling maximum located inside the ortho-1/2 phase region. In the tetra-0 and ortho-1/2 regions the agreement between the CMF results and the Monte Carlo data is excellent. The peak positions are close, but the CMF peak values somewhat exceed the nonscaling Monte Carlo maxima. We believe this disagreement in the tetra-0 phase is due to disruption of the one-dimensional fluctuations by orientational fluctuations of the chain fragments, which are not considered in the CMF approximation. Since, in contrast to the tetra-0 phase, the ortho-1/2 phase is orientationally ordered, the disruption is less severe there, leading to better agreement between the CMF and Monte Carlo results. The close agreement between the CMF results and the nonscaling maxima in the Monte Carlo data for C we take as a strong indication that these maxima are

caused by essentially one-dimensional local fluctuations associated with the formation of short fragments of oxygen chains in the disordered tetra-0 phase, and short “chains” of vacant oxygen sites in the ordered ortho-1/2 phase. The subsidiary maxima in the CMF data we interpret as nonscaling background contributions due to local fluctuations near the phase transitions themselves. These contributions are small compared with the scal-

ing maxima in the Monte Carlo data, which correspond to long-range critical fluctuations. We observe similar results in comparing the Monte Carlo and CMF results for the nonordering susceptibility, as well. In Fig. 2(b) we show $k_B T \chi_\Theta / N$ versus $\mu / |\Phi_{NN}|$. Single CMF maxima are located within the tetra-0 and ortho-1/2 phase regions, and they coincide with the nonscaling maxima in the Monte Carlo data. In addition, the latter exhibit distinct, scaling maxima at the phase transitions.

The positions in the phase diagram of the local-fluctuation maxima in C and χ_Θ are shown in Figs. 3 and 4, respectively. In both figures panel (a) displays the data in terms of temperature and chemical potential, and panel (b) in terms of temperature and oxygen concentration.

In Fig. 3 the specific-heat peak which lies in the tetra-0 phase region in Fig. 2(a) is seen to persist up to high temperatures. As T is increased, the peak moves towards smaller μ [panel (a)] and higher Θ [panel (b)], while its half width increases. The agreement with the Monte Carlo data is excellent for low T , and reasonable even at high T . The peak which lies in the ortho-1/2 phase region in Fig. 2(a) moves towards larger μ in a similar, but not quite symmetrical, fashion. The agreement between the CMF and Monte Carlo results remains closer than for the peak which lies in the tetra-0 phase, up to such temperatures where the Monte Carlo peak cannot be resolved from the scaling maximum at the tetra-0-to-ortho-1/2 phase transition. Surprisingly, the two smaller peaks, which at low T coincide with the phase transitions involving the ortho-1/4 phase, also persist up to temperatures considerably above the maximum critical temperature for this phase. Eventually they merge into one low maximum, centered at $\mu \simeq 0$ and $\Theta \simeq 0.25$, which can be detected in the Monte Carlo data, even at $k_B T / |\Phi_{NN}| = 0.45$.

In Fig. 4 the positions of the two local-fluctuation maxima in the nonordering susceptibility χ_Θ are seen to remain relatively constant at low T , whereas the peaks broaden, move together, and eventually merge as T is increased above the maximum critical temperature of the ortho-1/4 phase. An alternative way to define a disorder line is as the locus of points where the imaginary part of the largest complex eigenvalue of the transfer matrix vanishes.^{4,6,8} Some points where this condition is satisfied, obtained from a numerical transfer-matrix calculation with strip width $N=12$, are also indicated in Fig. 4. The finite-size effects are considerable, leading to a smaller separation between the disorder lines than indicated by the other two methods. This is particularly evident in the temperature range $k_B T / |\Phi_{NN}| \in [0.2, 0.3]$, probably due to the influence of the four-state Potts multicritical point, where the three lines of phase transitions merge.^{3,9} The general agreement between the CMF data and the numerical Monte Carlo and transfer-matrix results is good. In Fig. 4(b) are also included the position and approximate half width of the disorder peak observed by McKinnon *et al.*¹ at $T=923$ K. The qualitative agreement is good, but the difference in Θ between the disorder

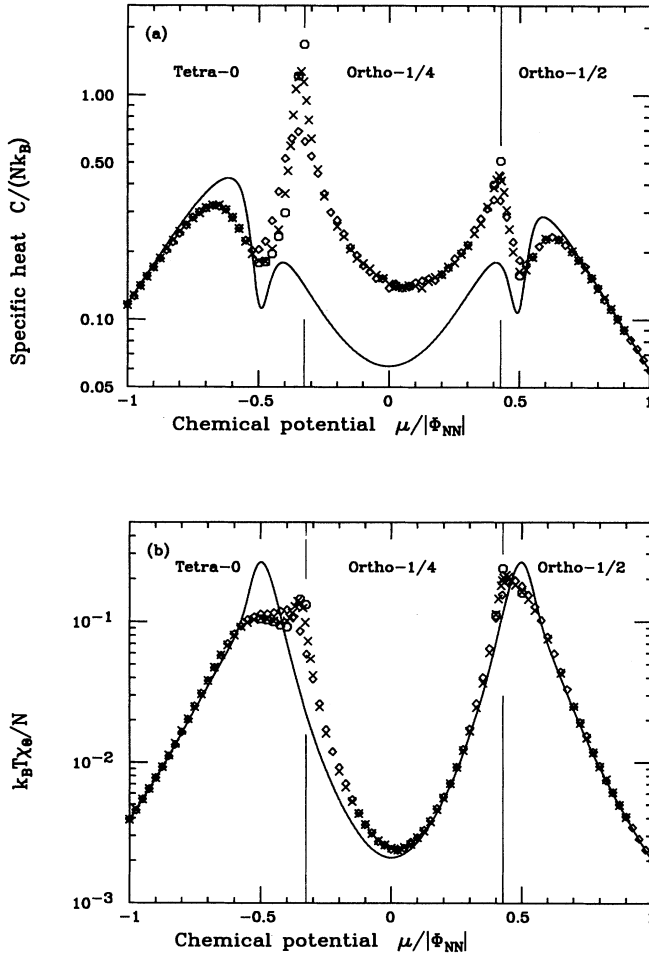


FIG. 2. The specific heat per site $C/(Nk_B)$ (a) and the nonordering susceptibility per site $k_B T \chi_\Theta / N$ (b) are shown vs chemical potential $\mu / |\Phi_{NN}|$ for the lattice-gas model with the dimensionless effective interactions $\Phi_{NN} = -1$ (repulsive), $\Phi_V = -0.5$ (repulsive), and $\Phi_{Cu} = +0.5$ (attractive). The temperature is $k_B T / |\Phi_{NN}| = 0.175$ (approximately 640 K). The solid lines represent the contributions from local fluctuations, obtained with our CMF method, whereas the data points are Monte Carlo results for the full specific heat and nonordering susceptibility of $2(L \times L)$ systems with $L = 8$ (\diamond), 16 (\times), and 32 (\circ). The vertical lines mark the phase transitions that separate the three phases, tetra-0, ortho-1/4, and ortho-1/2. They were obtained by numerical transfer-matrix finite-size scaling calculations with $N/N' = 8/12$ (Ref. 3). See the detailed discussion in the text.

der peak and the peak which corresponds to the phase transition is smaller than predicted.

As can be seen from the ground-state diagram [Fig. 2(b) of Ref. 3], the distance between the disorder peak and the peak which corresponds to the phase transition is an approximate measure of the strength of

the chain-chain repulsion Φ_V . We have therefore also calculated χ_Θ at $T=923$ K, using the effective interactions recently obtained by Sterne and Wille with the LMTO method.²³ These are $\Phi_{NN} = -27.6$ mRy, $\Phi_{Cu} = +9.6$ mRy, and $\Phi_V = -4.4$ mRy. The position of the tetra-0-to-ortho-1/2 phase transition for these interactions has

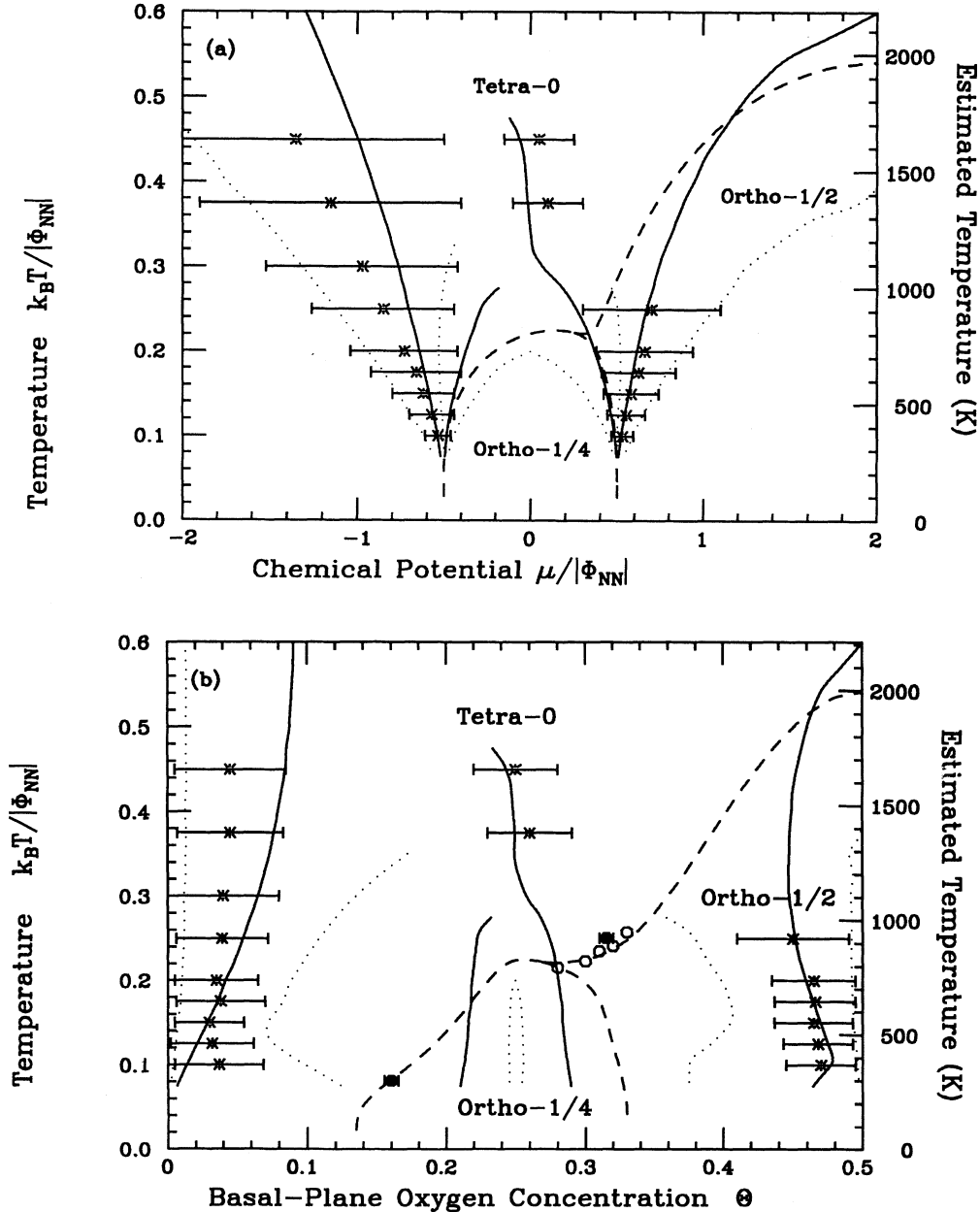


FIG. 3. We show the positions of the local-fluctuation peaks in the specific heat C , obtained with our CMF approximation (solid lines), and their approximate half widths at half maximum (dotted lines). The positions of the nonscaling maxima in the Monte Carlo data for C are also shown (*), with approximate half widths indicated as horizontal error bars. The lattice-gas interaction constants are the same as in Fig. 2. For reference are shown the phase boundaries obtained by numerical transfer-matrix calculations with $N/N' = 8/12$ (Ref. 3) (dashed lines). (a) displays the data in terms of temperature $k_B T / |\Phi_{NN}|$ vs chemical potential $\mu / |\Phi_{NN}|$. (b) displays the same data in terms of $k_B T / |\Phi_{NN}|$ vs basal-plane oxygen concentration Θ . Here are also shown experimental points for the locations of the phase boundaries from Specht *et al.* (Ref. 22) (o), which are used to establish the estimated temperature scale along the right-hand vertical axes, and from McKinnon *et al.* (Ref. 1) (•).

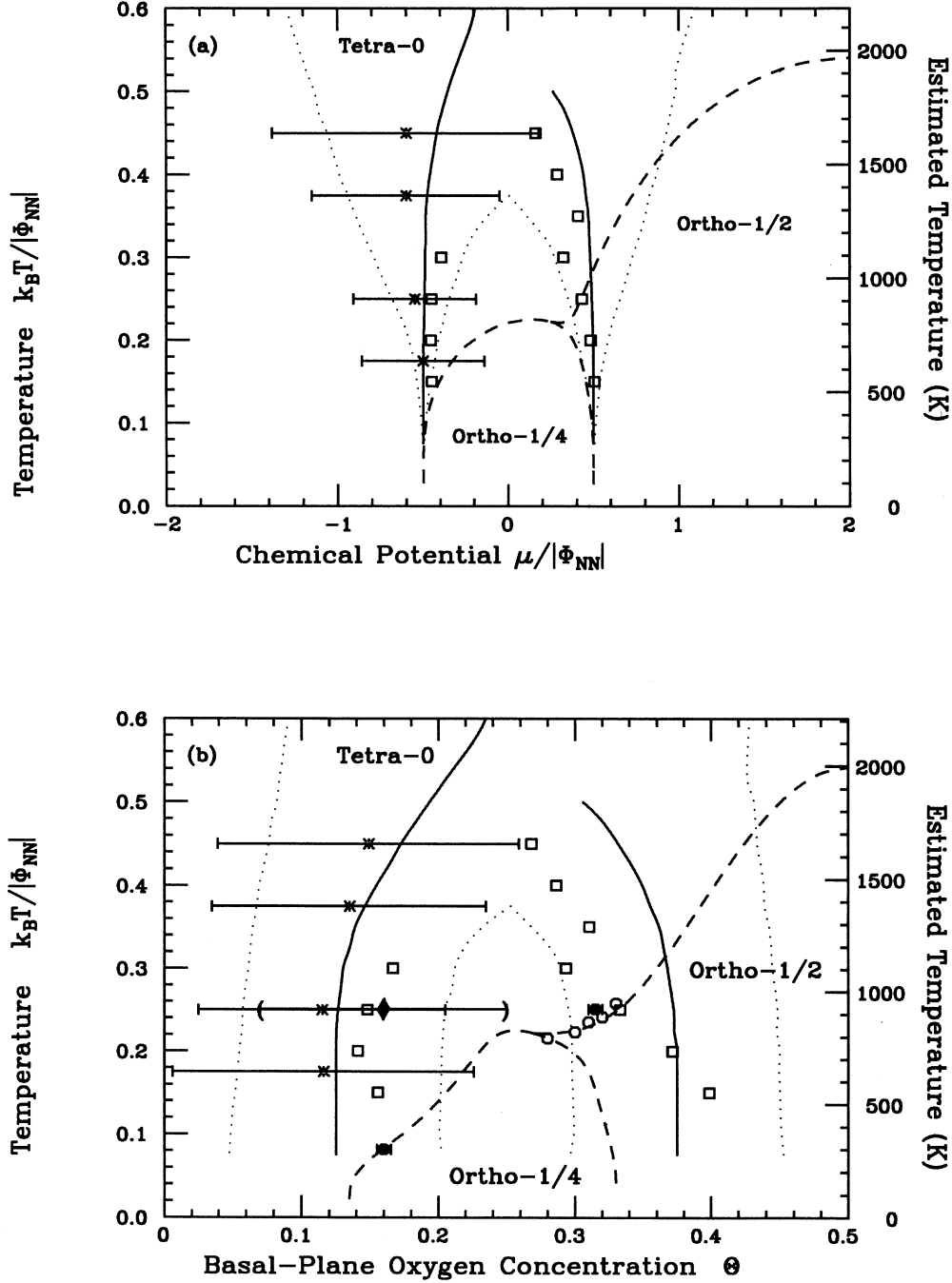


FIG. 4. We show the positions of the local-fluctuation peaks in the nonordering susceptibility χ_Θ . The interactions are the same as in the previous figures, and the solid, dotted, and dashed lines have the same interpretations as in Fig. 3. The positions of the nonscaling maxima in the Monte Carlo data are shown (*), with approximate half widths indicated as horizontal error bars. As an independent estimate of the positions of the disorder lines (Refs. 4, 6, and 8), points where the imaginary part of the largest complex eigenvalue of the transfer matrix vanishes for a system of size $N=12$ are also shown (\square). The finite-size effects in this estimate are considerable, leading to a smaller separation between the disorder lines than obtained by the other two methods. (a) displays the data in terms of $k_B T / |\Phi_{NN}|$ vs $\mu / |\Phi_{NN}|$. (b) displays the same data in terms of $k_B T / |\Phi_{NN}|$ vs Θ . The experimental points representing the phase boundaries are the same as in Fig. 3(b). In addition we show the position (solid diamond) and approximate half width (horizontal error bar with crescent-shaped ends) of the disorder peak in χ_Θ , observed by McKinnon *et al.* (Ref. 1).

been determined by a transfer-matrix finite-size scaling calculation with $N/N' = 8/12$.²⁹ In Fig. 5 the experimental and numerical results are shown together as functions of Θ . Two distinct maxima are seen in this figure: The one to the left is the disorder-line peak in the tetra-0 phase, whereas the one to the right is a superposition of the phase-transition peak and the disorder-line peak in the ortho-1/2 phase, which lie too close to be resolved. We emphasize that no adjustable parameters have been used. The agreement between the experimental and numerical data is striking, especially for the peak positions and the height of the disorder maximum in the tetra-0 phase. The fact that the experimental peak near the phase transition is lower and less sharp than the scaling Monte Carlo peak, we believe is due to the finite experimental resolution, and possibly to sample inhomogeneities causing smearing of the transition.

A number of authors have proposed the existence of a separate, low-density orthorhombic phase at low temperatures.^{2,9-12} Such a phase, a one-dimensional dilute "gas" of completely filled parallel oxygen chains, would break the rotational, but not the translational, symmetry of the underlying lattice. To look for evidence of such a phase we have performed Monte Carlo simulations with Glauber dynamics of $2(L \times L)$ systems with $L=32$ at $k_B T/|\Phi_{NN}|=0.10$ and 0.05 . At the higher of these temperatures the system in the tetra-0 disordered phase was seen to consist of short chains of oxygen atoms, randomly dispersed and oriented. At the tetra-0-to-ortho-1/4 phase transition these chains were observed to order orientationally and pack into an ortho-1/4 (2×1) configuration with occasional breaks in the chains. This picture agrees completely with the result that this phase transition belongs to the XY universality class.^{3,9} The disorder maxima in the nonordering susceptibility and the specific heat are related to the fluctuations in the chain lengths. At the lower temperature, $k_B T/|\Phi_{NN}|=0.05$, the configurations that we observe on the low- μ side of the transition to the ortho-1/4 phase resemble the low-density orthorhombic phase described above. However, since the filled oxygen chains are sufficiently far apart to be treated as isolated Ising chains in an external field, the correlation length along the chains is easily calculated.²⁸ At $\mu/|\Phi_{NN}| = -0.5$ (near the disorder line) the correlation length is approximately 74, more than twice L . Because of the periodic boundary conditions, spanning chains are the rule whenever the correlation length is larger than about $L/2$. We therefore believe that the numerical data that have been taken as evidence of a low-density orthorhombic phase simply express finite-size effects due to the large correlation lengths.

In this work we have studied the macroscopically observable effects of local fluctuations near disorder lines in the phase diagram for a lattice-gas model of oxygen ordering in the high-temperature superconductor $\text{YBa}_2\text{Cu}_3\text{O}_{6+x}$. These effects are readily observable in experiments, as well as in numerical mean-field, Monte Carlo, and transfer-matrix calculations. We have devel-

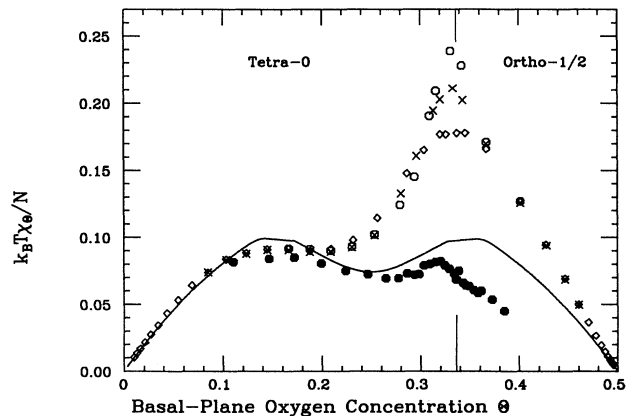


FIG. 5. The nonordering susceptibility $k_B T \chi_\Theta / N$ is shown vs oxygen concentration Θ at $T = 923$ K. The experimental data of McKinnon *et al.* (digitized from Fig. 4 of Ref. 1) are represented by solid circles. Numerical results are given for the lattice-gas model with the effective interactions obtained in LMTO calculations by Sterne and Wille (Ref. 23): $\Phi_{NN} = -27.6$ mRy, $\Phi_{Cu} = +9.6$ mRy, and $\Phi_V = -4.4$ mRy. The plotting symbols for the CVM and Monte Carlo numerical data are the same as in Fig. 2. The vertical lines mark the phase transition between the tetra-0 and ortho-1/2 phases, obtained by numerical transfer-matrix calculations with $N/N' = 8/12$ (Ref. 29).

oped a physical picture of these fluctuations in terms of randomly dispersed and oriented finite oxygen chains, and established that this picture enables us to obtain both the experimentally measured thermodynamic response functions, and an alternative to the low-density orthorhombic phase proposed by other authors.

Note added in proof. After this paper went to press P. Schleger kindly brought to our attention recent experimental data for χ_Θ at temperatures between 723 and 923 K [P. Schleger, W. N. Hardy, and B. X. Yang, *Physica C* (to be published)]. At 923 K these results are in reasonable agreement with those of Ref. 1, but indicate a somewhat smaller distance between the disorder- and phase-transition peaks over the whole temperature range.

ACKNOWLEDGMENTS

We thank D. de Fontaine, T. L. Einstein, D. P. Landau, W. R. McKinnon, M. Schick, P. A. Sterne, and L. T. Wille for useful discussions. Supported in part by the Florida State University Supercomputer Computations Research Institute, which is partly funded by the U.S. Department of Energy, Contract No. DE-FC05-85ER25000, and by FSU through time granted on its Control Data Corporation Cyber 205 and ETA Systems ETA-10 supercomputers. P.A.R. enjoyed the hospitality of the IBM Bergen Scientific Centre, and also acknowledges partial support by The Donors of the Petroleum Research Fund, administered by the American Chemical Society.

- ¹W. R. McKinnon, M. L. Post, L. S. Selwyn, G. Pleizier, J. M. Tarascon, P. Barboux, L. H. Greene, and G. W. Hull, *Phys. Rev. B* **38**, 6543 (1988).
- ²D. de Fontaine, M. E. Mann, and G. Ceder, *Phys. Rev. Lett.* **63**, 1300 (1989).
- ³T. Aukrust, M. A. Novotny, P. A. Rikvold, and D. P. Landau, *Phys. Rev. B* **41**, 8772 (1990).
- ⁴J. Stephenson, *J. Math. Phys.* **11**, 420 (1970).
- ⁵J. Stephenson, *Phys. Rev. B* **1**, 4405 (1970).
- ⁶R. Liebmann, *Statistical Mechanics of Periodic Frustrated Ising Systems*, Vol. 251 of *Lecture Notes in Physics* (Springer, Berlin, 1986).
- ⁷G. Gompper and M. Schick, *Chem. Phys. Lett.* **163**, 475 (1989); *Phys. Rev. Lett.* **62**, 1647 (1989); *Phys. Rev. B* **41**, 9148 (1990).
- ⁸G. Gompper and M. Schick, *Phys. Rev. A* **42**, 2137 (1990).
- ⁹N. C. Bartelt, T. L. Einstein, and L. T. Wille, *Phys. Rev. B* **40**, 10759 (1989).
- ¹⁰R. Kikuchi and J.-S. Choi, *Physica C* **160**, 347 (1989).
- ¹¹D. de Fontaine, G. Ceder, and M. Asta, *Nature* **343**, 544 (1990).
- ¹²G. Ceder, M. Asta, W. C. Carter, M. Kraitchman, D. de Fontaine, M. E. Mann, and M. Sluiter, *Phys. Rev. B* **41**, 8698 (1990).
- ¹³D. de Fontaine, L. T. Wille, and S. C. Moss, *Phys. Rev. B* **36**, 5709 (1987).
- ¹⁴L. T. Wille, A. Berera, and D. de Fontaine, *Phys. Rev. Lett.* **60**, 1065 (1988).
- ¹⁵L. T. Wille and D. de Fontaine, *Phys. Rev. B* **37**, 2227 (1988).
- ¹⁶A. Berera, L. T. Wille, and D. de Fontaine, *J. Stat. Phys.* **50**, 1245 (1988).
- ¹⁷A. Berera, L. T. Wille, and D. de Fontaine, *Physica C* **153-155**, 598 (1988).
- ¹⁸Z.-X. Cai and S. D. Mahanti, *Solid State Commun.* **67**, 287 (1988).
- ¹⁹Z.-X. Cai and S. D. Mahanti, *Phys. Rev. B* **40**, 6563 (1989).
- ²⁰L. T. Wille, *Phase Trans. B* **22**, 225 (1990).
- ²¹R. Beyers and T. Shaw, in *Solid State Physics*, edited by H. Ehrenreich and D. Turnbull (Academic, New York, 1989), Vol. 34, p. 135-212.
- ²²E. D. Specht, C. J. Sparks, A. G. Dhere, J. Brynestad, O. B. Cavin, D. M. Kroeger, and H. A. Oye, *Phys. Rev. B* **37**, 7426 (1988).
- ²³P. A. Sterne and L. T. Wille, *Physica C* (to be published).
- ²⁴D. J. Scalapino, Y. Imry, and P. Pincus, *Phys. Rev. B* **11**, 2042 (1975).
- ²⁵J. Chalupa and M. R. Giri, *Solid State Commun.* **29**, 313 (1979).
- ²⁶C. P. Landee, R. E. Greeney, W. M. Reiff, J. H. Zhang, J. Chalupa, and M. A. Novotny, *J. Appl. Phys.* **57**, 3343 (1985).
- ²⁷J. Chalupa and M. A. Novotny, *Solid State Commun.* **54**, 843 (1985).
- ²⁸R. J. Baxter, *Exactly Solved Models in Statistical Mechanics* (Academic, London, 1982), p. 34. This standard reference gives the equivalent result for the magnetization M of the one-dimensional Ising model in magnetic field H . Equation (5) is obtained by the transformations $M = 2\tilde{E} - 1$, $H = (\mu_\alpha - \mu_0)/2$.
- ²⁹D. Hilton, B. Gorman, P. A. Rikvold, and M. A. Novotny, *Phys. Rev. B* (to be published).